2.E Radial Compression of Picosecond Electrical Pulses

Introduction

Acceleration of electrons and positrons in conventional rf linacs is presently limited to gradients of order 20 MV/m. To extend e^+e^- collisions to the TeV region, it is necessary to achieve gradients at least an order of magnitude larger, and several promising proposals are being explored.[1-3] The high electric field at the focus of intense lasers[4] provides a suitable gradient, but so far no practical geometry has been found for efficient particle acceleration.

Recently, Willis[5] suggested the use of ultrafast lasers to switch power from a DC high-voltage source onto an accelerating structure. The proposed structure consists of circular discs and thus acts as a radial transformer. If the rise time of the electrical pulse is of the order of the gap spacing (~ 1 mm), a voltage gain of a factor of 10 can be achieved. Furthermore, because of the small gap spacing a very high gradient is, in principle, attainable.

Radial compression of electrical pulses had been considered[6] in the 1960s and is used in accelerators such as the particle-beam fusion accelerator (PBFA);[7] recent studies on a large-scale model have been reported by Aronson et al.[8] A compact structure is needed for a high-energy accelerator; this has now become possible because of the availability of fast-pulsed lasers for driving the high-voltage switch. Willis and his group are working on laser-triggered photoemission from a wire cathode;[9] Villa[10] proposed a laser-triggered spark gap. Here we report on results obtained using photoconductive switching of high-resistivity silicon.

Using a high-power picosecond laser developed at LLE,[11] we were able to demonstrate voltage gain in a structure with an outer radius $R = 3$ cm and gap $g = 2$ mm. Since the field at the center of the disc must be measured with picosecond time resolution, we measured the electro-optic effect and sampled the waveform by delaying the optical probe.[10] A hard tube pulser provided the high voltage that was applied on the outer diameter of the discs 10 ns–100 ns before switching. The observed waveforms and their amplitude are in qualitative agreement with the calculated values.

Prototype Structure

The structure used in this investigation is shown in Fig. 32.20. The lower brass disk is grounded and the upper disc is a silicon wafer 500-μm thick. A gold coating on the inner side of the silicon serves as the "anode" to provide the conducting structure in which the pulse propagates. A ring of gold coating, connected to the high-voltage feed, was deposited on the other side of the silicon at its outer circumference. The two discs were separated by 2 mm and had a 1-mm-diameter hole at their center. A 2-mm-thick KDP crystal was placed at the center; it had dimensions 1×1 mm^2 and had a reflective coating on one side and it was probed in reflection.
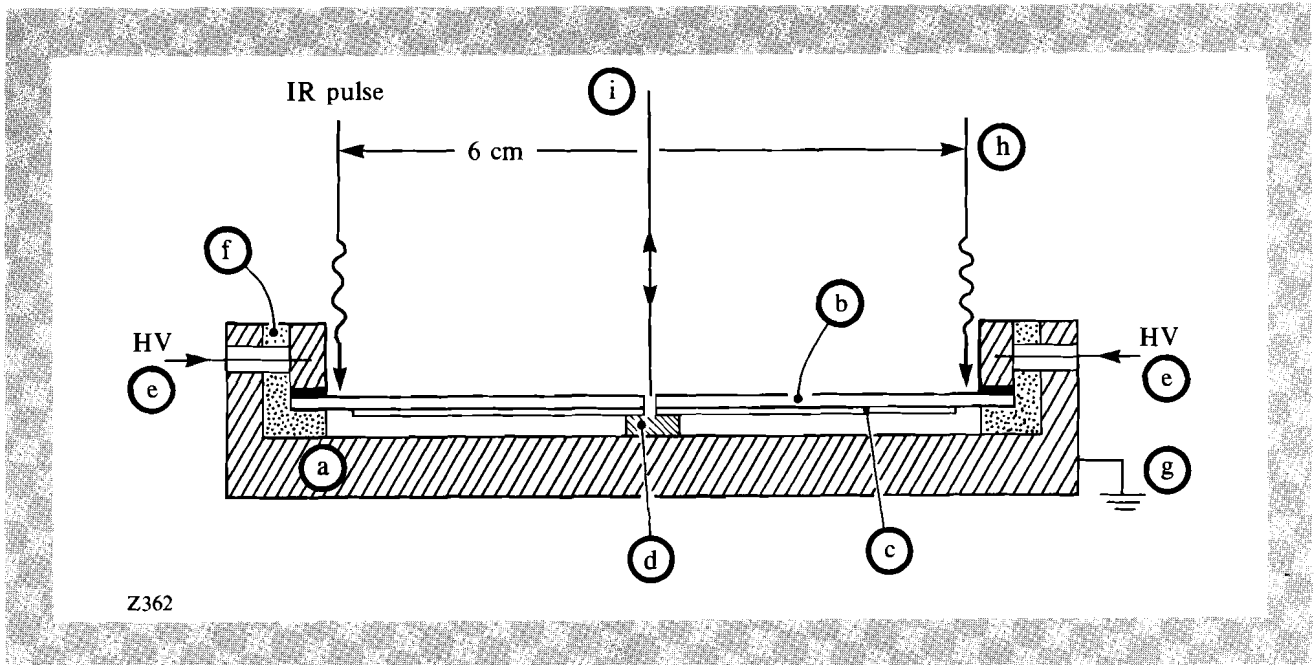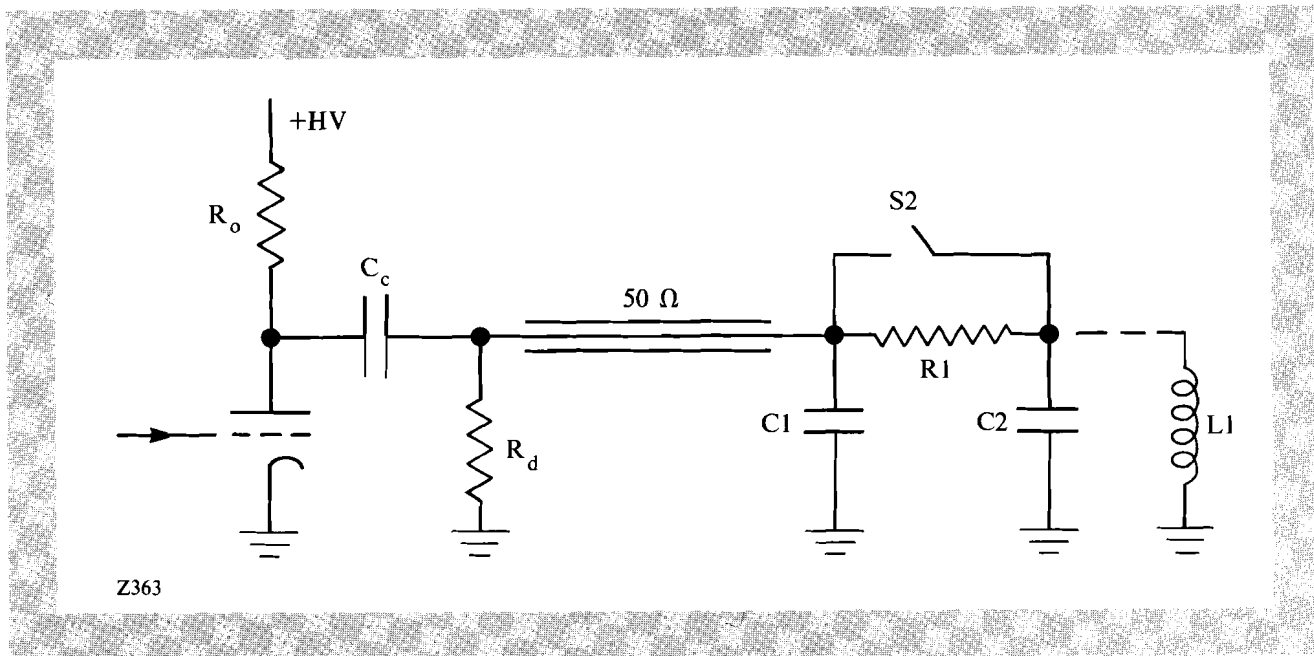
Fig. 32.20
Cross section of the disc structure:
(a) cathode brass disc; (b) silicon
wafer; (c) gold coating; (d) KDP
crystal; (e) HV feed; (f) insulator; (g)
ground; (h) IR pulse; and (i) probe
pulse.

Fig. 32.21
The equivalent circuit for the
structure.

The equivalent electric circuit is shown in Fig. 32.21. The disc
structure is represented by C2, even though at these speeds it is a
distributed system; C1 is the charging capacity; C1 $\sim$ 20 pF; and R1
represents the ohmic impedance across the silicon disc between the
conducting coatings R1 $\sim$ 10kΩ (ρ = 7kΩ-cm). S2 represents the
photoconductive (ρ = 7kΩ-cm) switch, which shorts R1. When the
charging pulse $-V_o$ is applied at C1, the upper plate of C2 floats
toward $-V_o$, charging up C2; to prevent this, a small conducting
spring, indicated by the inductance L1, was inserted between the discs.

The waveform at the charging electrode (i.e., the C1, R1 node) is shown in Fig. 32.22(a). Because of the impedance mismatch, the voltage builds up to $-V_o$ by successive reflections; the IR switching beam is blocked. Figure 32.22(b) shows the waveform when switching takes place by the IR pulse, whose timing is indicated on the lower trace.

The impedance seen by the electrical pulse that propagates between the two disks is a function of the radius r; it is given approximately by $Z(r) = (377\ \Omega)(g/2\pi r)$, with g the gap spacing. For constant power, the voltage squared is proportional to the impedance, so that a gain of order $V(r_o)/V_o = \sqrt{R/r_o}$, where r_0 is the radius of the central aperture, can be expected. The propagation of a pulse of finite rise time can be calculated analytically,[10] obtaining for the voltage at the center of the discs

$$V_c = 2V_o\sqrt{\frac{2R}{g+c\tau_R}}$$ (1)

Here, V_o is the voltage at radius R and τ_R is the rise time of the pulse. Equation (1) shows the importance of ultrafast switching in maintaining a small gap between the discs.

Z364

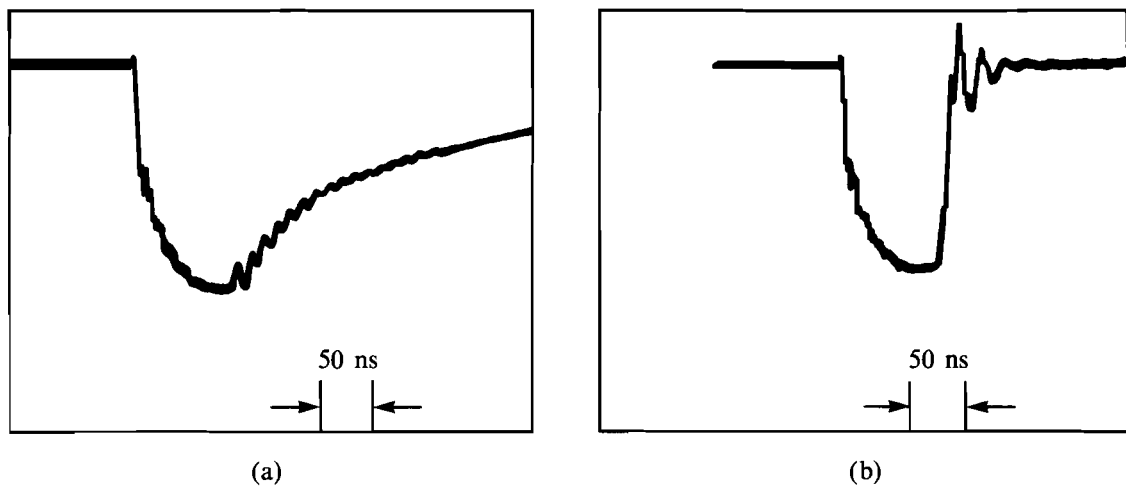(a)   (b)

Fig. 32.22
The waveform at the HV feed point:
(a) without switching, (b) with switching.

Optical System
The pulsed laser used in this investigation was a combination of a Nd:YLF oscillator and a Nd:glass amplifier ($\lambda = 1.054\ \mu$m), producing pulses of a few millijoules of 1-ps to 3-ps duration[11] at a repetition rate of 5 Hz. Pulses from a Nd:YLF mode-locked oscillator are stretched to 300 ps, chirped in a 1.5-km optical fiber, and injected into a regenerative amplifier. The pulse is amplified to saturation and

ejected from the optical cavity. The final pulse retains its chirp. Reflection gratings, arranged to compensate for the optical chirp, compress the pulse to 1 ps. This sequence is shown schematically in Fig. 32.23.

The spatial profile of the IR pulse was modified by an optical system incorporating a toroidal lens. The annulus of IR light was focused onto the silicon switch at the periphery of the radial transmission line. The attenuation length at $\lambda = 1.054$ μm is of the order of 1 mm, so that carriers are being produced throughout the bulk of the silicon wafer. A fraction of the pulse was split off, frequency doubled, and used to probe the electro-optic KDP crystal located at the center of the discs. A variable delay line in the pump beam provided the temporal scanning.
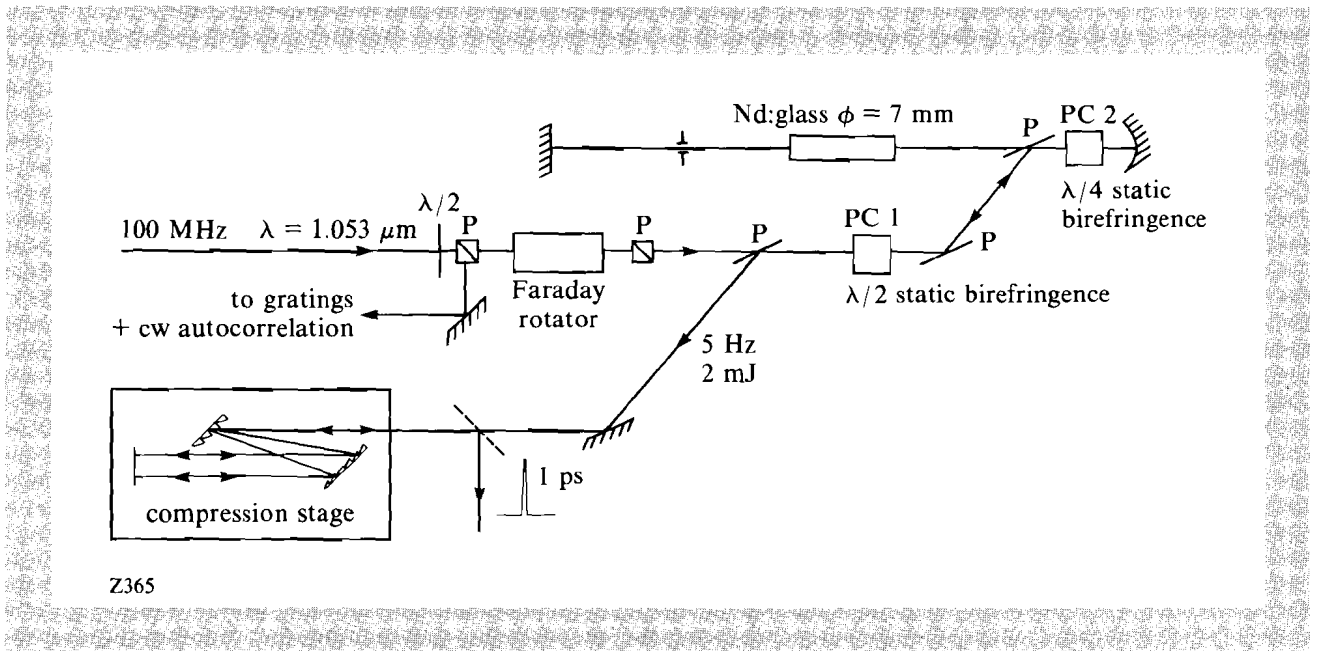

Fig. 32.23
Schematic of optical pulse
amplification and compression.

The sampling system is shown schematically in Fig. 32.24. The frequency-doubled green beam is passed through a Glan-Thompson polarizer, followed by a compensator (variable retardation device), so that elliptically polarized light is incident on the electro-optic crystal. This crystal has the property that its birefringence changes in response to an applied electric field, thus changing the polarization of the light. After reflection, the beam retraces its path, and the component orthogonal to the original polarization direction is detected by a photodiode. The compensator is set so that after the double transversal the light is circularly polarized and the detector is biased to half of maximum intensity.

The electro-optic effect was longitudinal and thus independent of crystal thickness, yielding a half-wave voltage[12] $V_\pi = 10$ kV at $\lambda \sim 530$ nm. To improve signal to noise, the electrical pulse was applied on every second laser pulse, and the difference between 20 consecutive pulses was averaged in a boxcar integrator. Furthermore,
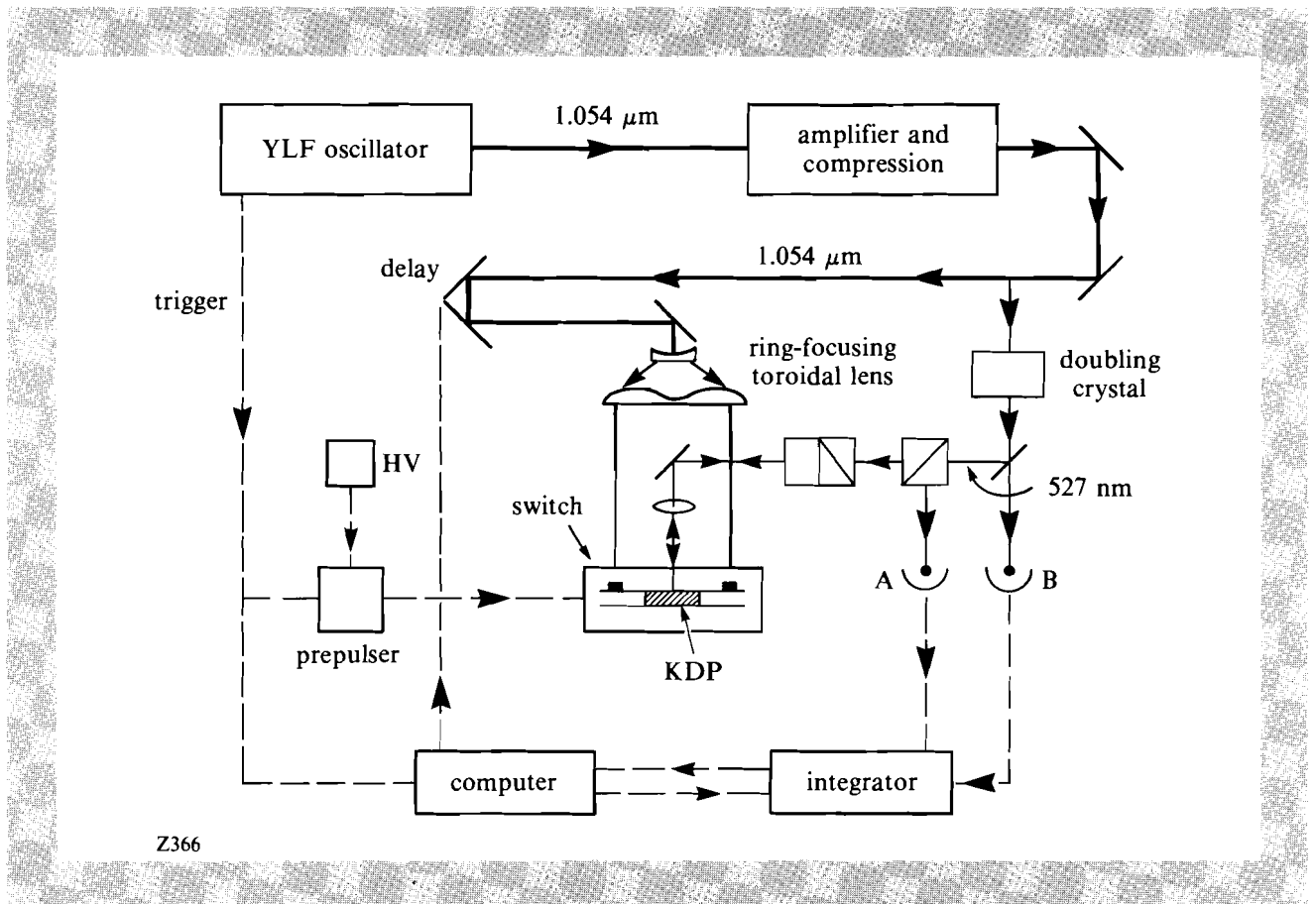
Fig. 32.24
Schematic arrangement of the electro-optic sampling.

Z366

the incident-pulse intensity was monitored and used for normalization. The output of the laser varies significantly from pulse to pulse, thus, it is necessary to use averaging techniques. The crystal was calibrated by applying a (quasi) static voltage (1.5 kV) across the discs. The results are shown in Fig. 32.25 and correspond to a bias $\phi = 0°$, 45°, and 90°, respectively. At 45°, the rotation induced by the voltage pulse, which is applied for every second laser pulse, is clearly shown as a distinct trace. At 0° and 90°, the signal is quadratic in the optical rotation angle and beyond our resolution.

When fast switching is desired, it is important to prevent any type of prepulses from accompanying the main pulse. The prepulses bleed the voltage across the switch and can completely distort the rise time of the electrical pulse. Evidence for such prepulses can be seen in the trailing edge of the waveform of Fig. 32.22(b). The optical delay line had a travel of 9.4 cm and a step size of 6.25 μm. Data points were taken every 25 steps, or 1.04 ps. However, the time resolution of the system is set by the thickness of the crystal. Since the probe beam traverses the 2-mm-thick crystal twice, given a refractive index n = 1.5, the resolution is of the order of $\delta t = 18$ ps.

Results

In our first measurements, a Teflon insert ~1.5 cm in diameter was used to hold the crystal in the center of the discs. This insert produced

significant reflections and had to be removed. Distortions of the waveform were also seen in connection with prepulses; these were reduced by tuning the laser. The best waveform observed is shown in Fig. 32.26.
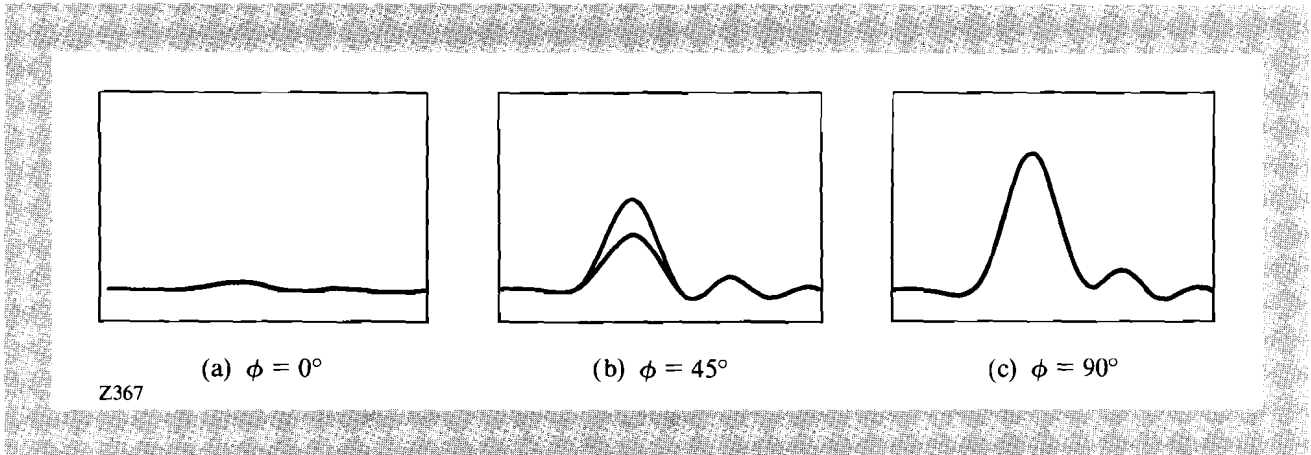

(a) $\phi = 0°$ (b) $\phi = 45°$ (c) $\phi = 90°$

Z367

Fig. 32.25
Calibration of the electro-optic effect. The voltage is applied only for every second laser pulse. (a) Bias $\phi = 0°$; (b) bias $\phi = 45°$; (c) bias $\phi = 90°$. At $\phi = 45°$, the signal is proportional to Γ, the optical rotation; at $\phi = 0°$, $90°$ it is proportional to Γ^2 and therefore too small to be observed.
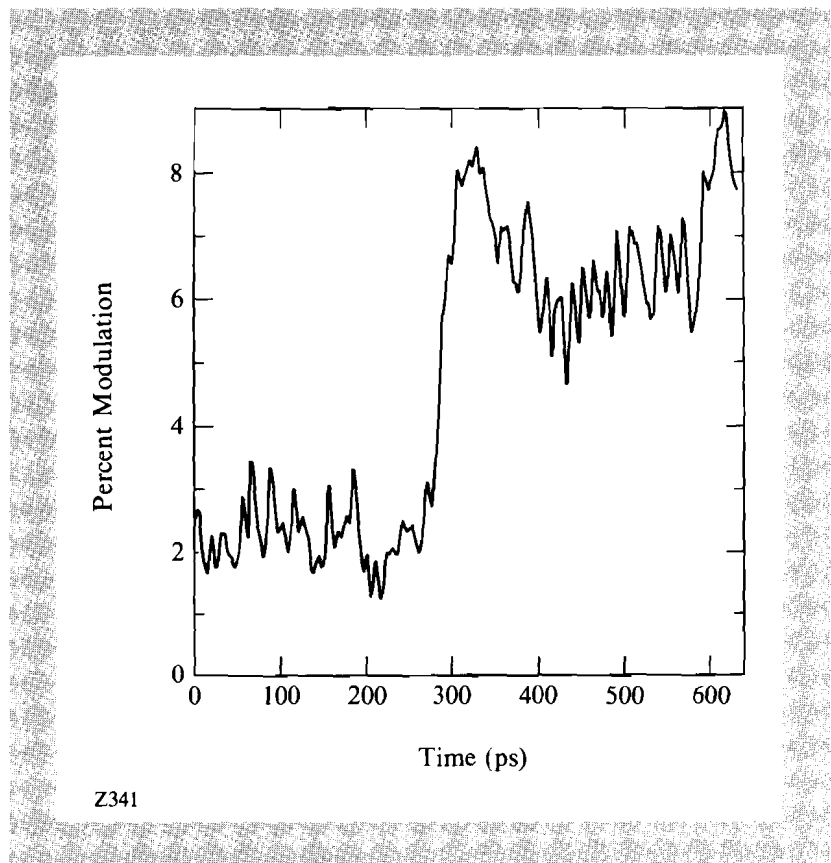

Time (ps)

Z341

Fig. 32.26
The waveform observed at the center of the discs. The observed rise time is 24 ps but the resolution is 18 ps.
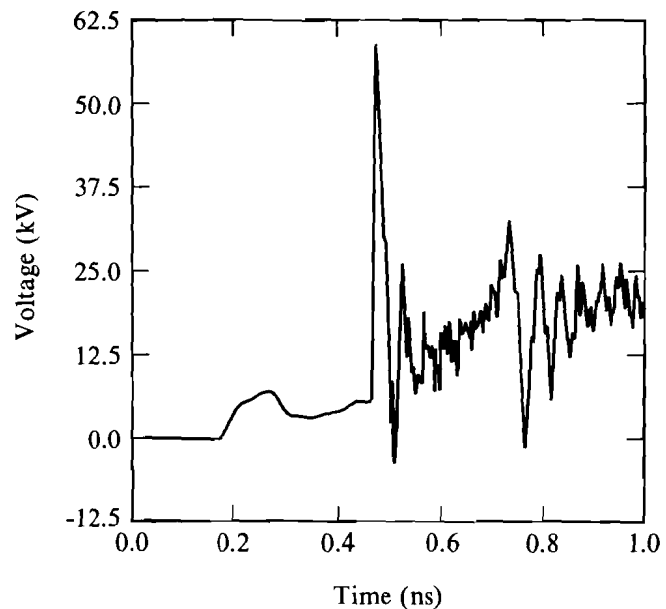
173

The measured rise time (10%-90%) is τ_M = 24 ps; this is a convolution of the actual rise time with the time resolution of the probe, δt = 18 ps. By simple quadrature, the true rise time is τ_R = 16 ps, and it is therefore probable that the peak amplitude exceeds the measured value by a factor of 1.5-2.0. A reflected pulse appears ~300 ps after the initial pulse. This corresponds roughly to the transit time for the round trip from the center of the disc to the edge of the structure and back (8 cm).

Based on the calibration of the crystal, the observed peak field is V_c = 1.0 kV. The charging voltage was V_o = 480 V, so that the observed gain is V_c/V_o ~ 2. To predict the gain from Eq. (1), we use τ_R = 16 ps, R = 3 cm, and g = 0.2 cm. The calculated gain is then

$$V_c = 2V_o\sqrt{8.8} = 5.9 \ V_o \ . \qquad (2)$$

Even if we take into account that (because of the resolution) the voltage at the center of the disc exceeds the observed V_c, the predicted value is greater than the observed value. This is probably due to reflections off the sampling crystal.

The propagation of the pulse on the structure has been calculated in detail by R. Barker, using a numerical integration code.[13] In that model, the silicon switch was closed with a 0.5-ps rise time and the measurements have not been smeared by finite resolution. The fields are calculated as a function of radius and time; Fig. 32.27 shows the waveform at the center. We note that in spite of the effects of

Fig. 32.27
The waveform at the center of the discs, as calculated in Ref. 13 for 0.5-ps rise time of the switch. Note the qualitative agreement with the observed data.

Z368

experimental resolution, the calculated waveform matches the observation very closely. The gain calculated by the numerical code is $V_c/V_o = 11$, in agreement with Eq. (1) for $\tau_R = 0$, $g = 1$ mm.

In conclusion, we have demonstrated that we can generate kilovolt electrical pulses with rise time $\tau_R = 16$ ps using a circular photoconductive switch. The propagation of this circular pulse toward the center gives rise to voltage gain in reasonable agreement with calculation. The energy in the switching pulse used for this investigation was ~1 mJ; we did, however, observe successful switching at significantly lower power levels as well.

Our present goal is to improve these measurements and observe gain of order ~10, while also increasing the supply voltage to a few tens of kV. We can then attempt to accelerate electrons photoemitted from the cathode; in that case, the KDP crystal is removed and the probe beam is frequency doubled once more so that the cathode is illuminated by a UV pulse. We believe that we can achieve gradients of 0.2 MV/mm–0.5 MV/mm and that one can stack several discs to make a structure of finite length. Such a device would make an electron source of high brilliance and could eventually be used for acceleration to TeV energies.

ACKNOWLEDGMENT

REFERENCES

1. A. M. Sessler and S. S. Yu, *Phys. Rev. Lett.* **58**, 2439 (1987).

2. T. Tajima and J. M. Dawson, *Phys. Rev. Lett.* **43**, 267 (1969).

3. G. A. Voss and T. Weiland, DESY Report 82-074 (1982); T. Weiland, *IEEE Trans. Nucl. Sci.* NS32, 3471 (1985).

4. K. Shimoda, *Appl. Opt.* **1**, 33 (1962).

5. W. Willis, "Switched-power Linac," CERN internal note EP/WJW/mm-0151D-1984.

6. E. C. Hartwig, "Pulsed line acceleration of electron rings," University of California preprint S/ERA-4, 1968.

7. See, for instance, B. N. Turman *et al.*, *Proc. of the 5th IEEE Pulsed Power Conference* (IEEE, New York, 1985), p.155.

8. S. Aronson, F. Caspers, H. Haseroth, J. Knott, and W. Willis, paper presented at the Washington, DC, Acceleration Conference, March 1987.

9. T. Rao and J. Fisher, BNL Instrumentation Division (private communication).

10. R. E. Cassell and F. Villa, "Study of a high gradient pulsed linac structure," SLAC-PUB-3804 (October 1985); also F. Villa, "High gradient linac prototype: A modest proposal," SLAC-PUB-3875 (January 1986).

11. D. Strickland and G. Mourou, *Opt. Commun.* **55**, 447 (1985).

12. In reflection, the half-wave voltage is one half of the value given.

13. R. J. Barker (private communication). The code "MAGIC" was used.